THE STRENGTH OF COMPOSITE POLYAMIDE WITH DIFFERENT MOLDING ORIENTATION UNDER HIGH STRAIN TENSION LOAD

By:

ARVIND DAYVAA A/L JEGANATHAN

(Matrix No: 140067)

Supervisor:

IR. DR. FEIZAL YUSOF

July 2020

This dissertation is submitted to

Universiti Sains Malaysia

As partial fulfilment of the requirement to graduate with honors degree in

BACHELOR OF ENGINEERING (MECHANICAL ENGINEERING)

School of Mechanical Engineering

Engineering Campus

Universiti Sains Malaysia

DECLARATION

I hereby declare that this work has not previously been accepted in substance for any degree and is not being concurrently submitted in candidature for any degree.

Signed:

(ARVIND DAYVAA A/L JEGANATHAN)

Date: 09/7/2021

Statement 1

The work reported in my thesis is the result of my own investigation, except where otherwise stated. Other sources are acknowledged by giving explicit references. Bibliography/references are appended.

Signed:

(ARVIND DAYVAA A/L JEGANATHAN)

Date: 09/7/2021

Statement 2

I hereby give consent for my thesis, if accepted, to be available for photocopy and for interlibrary loan, and for the title and summary to be made available outside organizations.

Signed:

(ARVIND DAYVAA A/L JEGANATHAN)

Date: 09/7/2021

ACKNOWLEDGEMENT

First and foremost, I want to express my gratitude to my supervisor, Ir. Dr. Feizal Yusof, for his help and direction during this research. He had given me a lot of helpful guidance on the philosophy underlying the project, thesis writing, and research paper preparation. Working with him has been a great experience, and I've learnt a lot from him over the making of this research.

In furthermore, I'd want to express my gratitude to Dr. Muhammad Fauzinizam Bin Razali, the coordinator of EMD 452, for his assistance in developing criteria for conducting research and preparing this thesis. Dr. Fauzinizam also organised a series of workshops to help students prepare their thesis. Next, I'd like to express my gratitude to En. Fakruruzi, my assistant engineer, who assisted me greatly with the setup of mechanical components and conducting the experiment. In addition, the assistance supplied by assistant engineers in the workshop is greatly valued. They had given me a lot of advice on how to use tools and machinery so that I could finish my final year project on time.

Finally, I'd want to appreciate everyone who helped me finish this project, whether it was indirectly or directly.

TABLE OF CONTENTS   **PAGES**

LIST OF FIGURES

LIST OF TABLES

LIST OF SYMBOLS/ABBREVIATIONS

A_B	Cross sectional area of bar
As	Cross sectional area of specimen
A_{st}	Cross sectional area of striker
C_B	Wave velocity along bar
C_{st}	Wave velocity along striker
D	Inner diameter of pipe
E_B	Young Modulus of bar material
F_i	Force exerted on incident bar
F_s	Force exerted on specimen
F_{st}	Reaction force exerted on striker
L_S	Gauge length of specimen
L_{st}	Length of striker cylinder
P	Air pressure within the pressure tank
d_i	Inner diameter of striker
d_o	Outer diameter of striker
f	Friction factor
g	Gravitational acceleration
h_f	Head loss
l	Length of pipe
m_{st}	Mass of striker
v_{st}	Velocity of striker
v	Velocity of fluid along the pipe
ε	Specimen's strain
ε_r	Reflected strain
ε_i	Incident strain
ε_t	Transmitted strain
$\dot{\varepsilon}$	Strain rate
$\bar{\varepsilon}$	Average strain
ε_{true}	True strain
ρ	Density of bar material

ρ_{st}	Density of striker material
ρ_B	Density of bar material
σ	Engineering stress
σ_1	Stress at the incident end
σ_2	Stress at the transmission end
$\bar{\sigma}$	Average stress
σ_E	Engineering stress
σ_{true}	True stress
σ_{st}	Stress on striker
σ_i	Stress on incident bar
σ_s	Stress on specimen
σ_t	Transmitted stress
σ_{th}	Stress on thread
D_0	Outer diameter
$\sigma_\approx$	Longitudinal Stress Thin Walls Pressure Vessel
σ_h	Hoop Stress
v	Volume
d_m	Mean Diameter
GF	Gage factor
α	Ratio of cross-sectional area
β	Ratio of mechanical impedance
GFRP	Glass Fibre Reinforced Plastic
SHPB	Split Hopkinson Pressure Bar
DAQ	Data Acquisition
SEM	Scanning Electron Microscopy
UTM	Universal Testing Machine

ABSTRAK

Projek ini menyiasat kekuatan ciri-ciri spesimen akibat orientasi aliran serat yang pelbagai semasa proses acuan. Eksperimen ini dilakukan dengan menggunakan mesin SHPB yang telah dibangunkan di Pusat Pengajian Kejuruteraan Mekanikal USM.

Bahan bergred fungsional yang digunakan dalam eksperimen ini adalah poliamida komposit yang dikenali sebagai Grivory. Untuk mencirikan penyebaran pengisi dalam bahan, mikroskop elektron imbasan digunakan. Kawasan pengisi dikaji menggunakan mikroskopi elektron pengimbasan, dan kekuatan tegangan spesimen diuji menggunakan Mesin Uji Universal. SHPB digunakan dalam kajian ini untuk mengira kadar regangan spesimen. Sebagai tambahan, sistem pengumpulan data untuk pemprosesan dan analisis. Kelajuan penyerang yang diperlukan untuk mencapai kadar regangan $800s^{-1}$ adalah pada 10.1393 m/s. Tangki bertekanan yang dimampatkan diubah menjadi diameter yang lebih besar dari asal 0.0508m ke 0.1016m sehingga untuk meningkatkan isipadu udara untuk memberikan kelajuan yang lebih tinggi ke palang dalam ujian SHPB.

Berdasarkan nilai eksperimen, halaju penyerang ditentukan bahawa pemampat udara pada 9 Bar ialah 10.25 m/s. Ketika tangki tekanan dimodifikasi, sekarang dapat meningkatkan isipadu udara dan dengan itu meningkatkan kekuatan udara sebagai gantinya meningkatkan kecepatan bar insiden setelah penyerang menyerang landasan pada bar insiden. Ini bermaksud bahawa bahan tersebut mengalami tahap regangan $800s^{-1}$.

Terakhir, dari ujian UTM, tegangan maksimum bagi spesimen P ialah 107.03 MPa dengan beban maksimum 642.2 N dan tegangan maksimum bagi spesimen C ialah 64.2 MPa dengan beban maksimum 385.3 N. Pada tekanan 9 bar, pengujian tegangan kadar terikan tinggi yang dicapai oleh Spesimen P adalah 836.79 s^{-1}, pada puncak tekanan maksimum yang tinggi pada 41.25 MPa; untuk spesimen C, ujian tegangan kadar terikan tinggi adalah 803.555 s^{-1}, pada puncak tegasan maksimum yang tinggi pada 40.37 MPa. Berdasarkan keluk tegangan tegangan yang diperoleh menggunakan ujian SHPB, kita dapat menyimpulkan bahawa spesimen P memberikan kadar regangan yang lebih tinggi dibandingkan dengan Spesimen C.

ABSTRACT

This project investigates a functionally graded material characteristic strength as a result of different fibre flow orientations during the moulding process. The experiment is conducted using a SHPB machine which was designed and developed in the School of Mechanical Engineering USM.

The functionally graded material used in this work is a composite polyamide known as Grivory. To characterize the distribution of the fillers in the material, a scanning electron microscope were employed. Scanning electron microscopy is used to examine the filler region, and a Universal Testing Machine is used to evaluate the specimen's tensile strength. In this work, SHPB is used to determine the specimen's dynamic mechanical properties at high strain rate. In addition, a data collecting system for data processing and analysis has been developed to characterize the behaviour of the tested composite polyamide. It was determined that striker velocity to achieve strain rate of $800s^{-1}$ is at 10.1393 m/s. The compressed pressurised tank is modified to bigger diameter from original 0.0508m to 0.1016m so that to increase the air volume to give higher speed to the bars in the impact test.

Based on experimental value, the striker velocity provided by the air compressor at 9 Bar is 10.25 m/s. As the pressure tank is modified, it can now increase the volume of air into the gun barrel and hence increase the air force to the striker which in return increase the speed of incident bar after the striker strike the anvil on the incident bar. This means that the material is underwent strain rate of $800s^{-1}$.

Lastly, from the UTM test, the maximum tensile stress for specimen P is 107.03 MPa with load at maximum of 642.2 N and maximum tensile stress for specimen C is 64.2 MPa with load at maximum of 385.3 N. At the pressure of 9 bar, the high strain rate tensile testing achieve by the Specimen P is 836.79 s^{-1}, at the high peak of maximum stress at 41.25 MPa; for specimen C, the high strain rate tensile testing is 803.555 s^{-1}, at the high peak of maximum stress at 40.37 MPa. Based on the stress strain curve obtain using SHPB test, we can conclude that the specimen P give higher strain rate compare to Specimen C.

CHAPTER 1 : Introduction

1.1   Project Overview

Glass fibre reinforced plastic also known as Glass fibre reinforced polymer. This synthetic composite material has been in demand for decades due to its high strength, low weight, and corrosion resistant properties. Fibreglass is a synthetic composite material made up of extremely fine glass and plastic fibres. Glass Fibre Reinforced Plastic (GFRP) was first developed in the mid 1930's for high-temperature electrical application. In the composite industry, it is the largest segment. This composite material is a relatively low-cost material when compared to carbon and other metal fibre composites.

Wind energy, aviation and defence, construction, automotive, and other industries all have a significant demand for GFRP products. Composite materials combine the properties of two or more materials in ways that neither fibre nor matrix can attain on their own. Organic, polyester, thermostable, vinyl ester, phenolic, and epoxy resins were used in the matrix. Because it is versatile and cost-effective to manufacture, GFRP composite material may be easily tailored. In the construction sector, this property has a lot of potential for development. End customers are drawn to fibreglass because of its durability, thermal efficiency, and strength.

Grivory GV-4H natural is a 40 percent glass-fibre reinforced engineered thermoplastic material based on a semicrystalline Polyamide and partly aromatic copolyimide combination [1]. Grivory GV-4H is used for injection moulding technical items and has outstanding properties even after moisture absorption. High stiffness and strength, dimensional stability, little warpage, good chemical resistance, and a superb surface finish are all characteristics of Grivory GV-4H natural. Split Hopkinson pressure bars are used to measure the strength of injection moulded fibre reinforced composites that come in specimen c (cross-flow) and specimen p (parallel flow).

A Split Hopkinson Pressure Bar / Kolsky Bar is used to examine the material properties of high strain rate materials. In a SHPB system, a precision accelerator, incidence bar, transmission bar, and stopping mechanism are all aligned. The longitudinal wave travels from the incidence bar to the material sample under test. Typically, the specimen is placed between the incident and transmission bars. Due to impedance mismatches, some of the wave is reflected back into the incident bar

(measured by strain gauge) and portion of the wave is transmitted into the transmission bar (measured by strain gage). As the wave moves through the system, data is received from strain gauges on both the incident and transmission bars. Stress, strain, and strain rate are calculated using the data obtained by the strain gauges.

Fibre alignment patterns are used to evaluate the specimens' mechanical and physical properties. The experimental methodologies for dynamic loading are primarily classified according to the final parameters to be examined, which include tensile and the strain rate range experienced during testing [2]. In this experiment, the strength of fibre alignment and strain rate of Grivory specimens are observed with increases of the strain rate in the range of ($800s^{-1}$ to $1000s^{-1}$). The results will be used to compared the Grivory material molding type for the strain rates by using SHPB.

1.2   Problem Statement

Motorola Solutions came out with 2 types of injection moulded fibre reinforced composites from Grivory GV-4H material. The characteristic strength of fibre orientation can be identified using SHPB, SEM and UTM. The current limitation of SHPB machine available in the Applied Mechanics laboratory of Mechanical Engineering department can only provide strain rate up to $608s^{-1}$. Thus, it's unable to meet requirement of customer which are in the range of $800s^{-1}$ to $1000s^{-1}$. In order to solve this, the size of the pressure tank is increased which will be fabricated along with a portable air-compressor which can provide larger pressure of compressed air.

1.3   Project Objective

This research aims to
- Examine the fibre flow orientations and percentage of fillers of Grivory GV-4H material.
- To examine quasi static strain load of the Grivory material until failure
- To increase the strain rate of SHPB to $1000s^{-1}$.
- To measure the high strain rate performance of different moulded P and C Functionally Graded Materials.

1.4   Scope of Work

As the current SHPB machine can only provide strain rate up to 608s-1, the pressure tank is modified so that it can now increase the volume of air into the gun barrel and hence increase the air force to the striker which in return increase the speed of incident bar after the striker strike the anvil on the incident bar. The specimen is fitted between an incidence bar and a transmission bar in Split Hopkinson Pressure Bar. The infrared sensors are connected to an Arduino, which is then connected to a computer. When the incident compression wave hits the specimen, it propagates. A portion of the incident wave is reflected back through the bar at the interface, forming the reflected wave. The striker velocity is measured, and the strain signals are saved in an Excel spreadsheet. For post-processing, MATLAB is used to read the Excel file.

Next, a universal tensile machine is used to conduct the tensile test. The tensile grips are used to hold the specimen. Connect the sample to the extensometer. Separate the tensile grips at a steady rate to begin the test. The speed varies depending on the form of the specimen and might range from 0.05 to 20 inches per minute. The period between the commencement of the test and the break should be between 30 seconds and 5 minutes. After the sample break, finish the test (rupture). The ruptured specimen will be then undergoing scanning electron microscopy to analysis the fibre alignment.

The ruptured specimen P and C from the tensile test and original specimen P and C are undergo scanning electron microscopy analysis. The dog bone samples for analysis were split into three pieces. The face of the specimen block is completely smooth and polished after multiple shavings have been removed. If the specimen's glass transition temperature is more than 100°C, the polishing is carried out at room temperature. If the specimen's glass transition temperature is below room temperature, the polishing step is carried out at a temperature that is at least 10°C below the lowest glass transition temperature of the specimen. This is a crucial step in the specimen preparation process for determining the fibre orientation. The image is then analysed using image processing software to determine the area percentage.

3

CHAPTER 2 : Literature Review

2.1 Molded Polyamide Glass Fibres

The behaviour of thermoplastics is determined by their polymer structure, which can be separated into semi-crystalline and amorphous material types. When different polymer grades are used, different preparation adjustments are required because each polymer has its own material properties and behaves differently under similar conditions [3]. The non-Newtonian flow behaviour of thermoplastic materials is one of their most distinguishing characteristics. Viscosity diminishes as shear rates increase. The regularly realised fountain flow is created when the melt front at the focal point of the wall thickness flows ahead of the melt at the walls due to a change in viscosity as a component of shear rate. The viscosity of a polymer is also modified by fillers, which can increase or reduce viscosity, thermal conductivity, specific heat, shrinkage, and crystallinity depending on the type of filler and the amount of filler used [4].

The tendency of thermoplastics to shrink volumetrically throughout the cooling process is another prevalent feature. Despite this, shrinkage is frequently nonuniform. This is identified with their polymer structure and fillers, yet additionally reliant on processing choices and local mould temperatures, bringing about differential cooling. A hot melt is injected into a cold mould in a series of cycles during the injection moulding process. The multiplication of comparable cycles across a large number of cycles results in a quasi-steady state in which the mould maintains the same temperature changes throughout each cycle and produces substantially the same component quality throughout a manufacturing process.

Another feature of polymers is their viscoelastic nature and behaviour, which has a direct impact on their final mechanical properties. The stress field in the part can and will be influenced by the polymer's time and temperature dependence during the injection moulding cycle. The material's Young's modulus increases where the melt solidifies and remains low in the liquid zones. While the component is restricted by the mould during the cooling process, the differential cooling of the component will influence how close tensions are formed [5]. The limitation of the mould vanishes when the item is eliminated from the mould.

A fibre-reinforced material, on the other hand, will exhibit viscoelastic behaviour while also exhibiting anisotropic shrinkage. The use of fibres in polymer materials transfers some of the stress to the fibres, resulting in increased mechanical characteristics [6]. The sort of fibre, aspect ratio, fibre content and fibre length will influence the injection moulding process as shown in Figure 2.1. This differential shrinkage, as well as the final anisotropic strength and stiffness, will be produced by fibres orientated in the flow direction vs. cross-flow [7]. The final fibre orientation between the surface and centre portions of the wall thickness will not be the same across the whole section, resulting in multiaxial stress in the interior. The orientation of the fibres is also affected by molten material entering the void during packing.
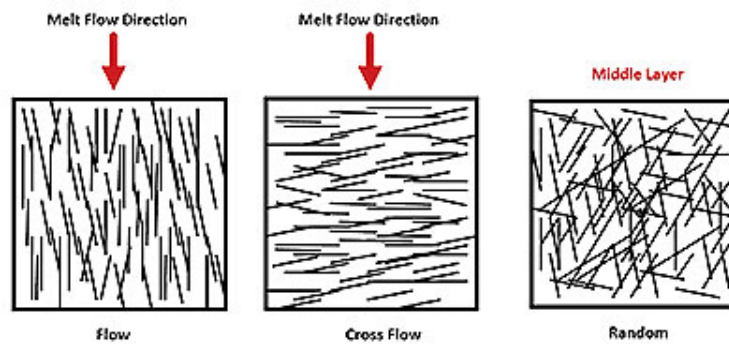
Figure 2.1: Flow of fibre orientation
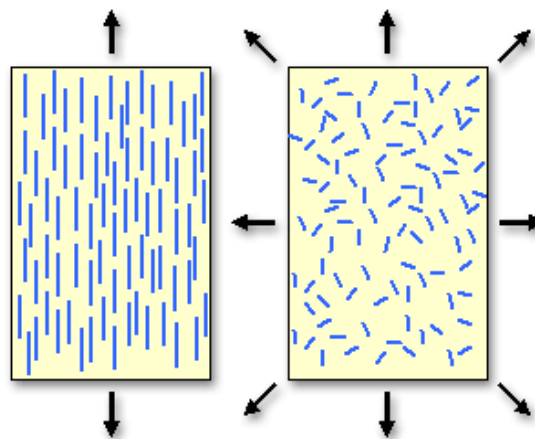
Figure 2.2: Different fibre orientation

The fibres in a composite can be aligned parallel to the loading direction to provide optimal strength and stiffness. When the force is applied perpendicular to the fibres, as shown in Figure 2.3, the composite may perform ineffectively [8].

To accommodate the direction of applied stress, fibres can be angled at 90°, 45°, or 30°.
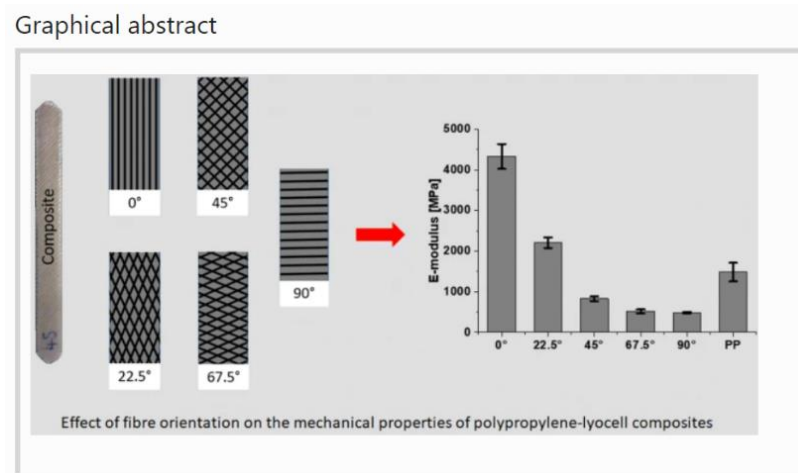
Figure 2.3: Orientation of fibres toward tensile direction.

Increasing the volume proportion of fibres in the composite results in increased stiffness and strength. However, there is an upper limit of about 80% fibres when the amount of matrix is insufficient to completely surround the fibres. Good bonding between the fibres and the matrix is required to ensure that load is adequately passed through the composite [9]. Bonding is also essential during the loading process to prevent the fibres from separating from the matrix. To increase bonding and moisture resistance, fibres are frequently treated with specific chemicals. The aspect ratio l/d is commonly used to describe fibres, where l is the fibre length and d is the fibre diameter.

For larger aspect ratios, i.e., a longer fibre or a smaller diameter, the composite qualities are frequently greater. The weight carried by the fibre's extremities is lower than the weight carried by the fibre's centre. There are disproportionately many ends in a composite made up of short fibres, indicating that the reinforcing is ineffective. Surface defects that induce brittle failure are less likely in smaller diameter fibres because they have less surface area [10].

To trace failure evolution, scanning electron microscopy (SEM) was utilized to assess morphological features on glass fibre reinforced polymer (GFRP) and epoxy resins before and after tensile tests. Prior to the tensile test, a micrograph analysis of

the GFRP plate reveals various intrinsic production faults that may impair the material's mechanical properties.

Each material's failure process was investigated, as well as the relationship between mechanical properties and material shape. Using a scanning electron microscope and optical microscopy, Jumahat developed a potential sequence of failure onset and progression of carbon fibre / toughened epoxy composites subjected to compressive pressure. According to the micrographs, the misaligned fibres failed in two points after reaching maximum micro-bending distortion, generating two planes of fracture to form a kink band [11].

Horst, J. J. and Spoormaker, J. L researched at fatigue fracture processes and fractography in polyamides with short glass fibre reinforcement [12]. Only a small fraction of fibres break owing to fatigue, he discovered, with the bulk of fibres being removed throughout the test. The degradation starts with the formation of vacancies, mainly around the fibre ends, which then combine into small cracks. M. Arif was evaluating multiscale fatigue damage in short glass fibre reinforced polymide-66 at various percentages of overall fatigue life using an X-ray micro-computed tomography (CT) technique on interrupted impact testing [13]. By examining void characteristics, he showed that damage builds constantly during fatigue loading and occurs along the fibre interface in the form of fibre/matrix interfacial debonding [14].

Due of the changes that composite materials and adhesive bonding materials exhibit over time, which are related to changes in the principal constituent, there is no mandated design code for composite materials and adhesive bonding materials in civil engineering. Following that, it's vital to focus on the principal constituent activity. Cohesive fracture is the desired failure mode in composite materials where an adhesive bonding is used to bind together two surfaces and a good adhesion between the matrix and the fibres that are used as loading carrying components is required.

2.1.1   Grivory GV-4H

The majority of today's adhesive bonding and composite materials research is focused on determining mechanical parameters such as glass transition temperatures and lap shear behaviour, using and developing a variety of approaches. The majority of investigations have not used Scanning Electron Microscopy (SEM) to assess the morphological features of the cross-section surface before and after failure. The purpose of this study is to perform SHPB to determine the specimen's strain rate, as

well as SEM to analyses the adhesive bonding cross section failure surface and the matrix-fibre interface in composite materials following a tensile test.

Nomenclature
Example, reinforced:

Grivory   G V - 5 H   black 9915
- Colour
- Heat stabilised
- 50%
- Reinforced with glass fibres
- Partially aromatic polyamide
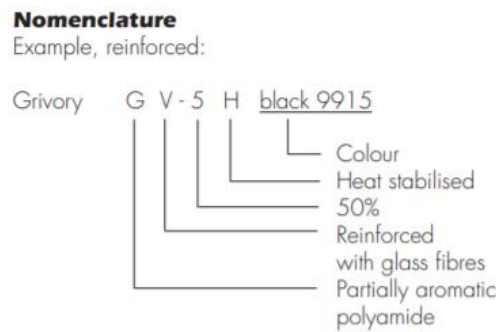
Figure 2.4: Grivory GV-4H nomenclature

Grivory® GV is the brand name for a series of engineering plastics that EMS GRIVORY manufactures [1]. This group of materials is made up of semi-crystalline polyamides with a small amount of partly aromatic component. Grivory GV is offered as a granular product for injection moulding in commonly used machinery and moulds. Figure 2.5 shows that Grivory GV-4H Natural has a glass fibre reinforcing content of 40% by weight in injection moulding grades. Grivory GV-4H Natural are stiff and strong even after absorption of moisture.

Grade	Grivory	Characteristics and properties	Processing / application segment
Basic grades	GV-2H GV-4H GV-5H GV-6H	Injection moulding grades with 20 – 60% by weight glass fibre reinforcement. Stiff and strong, even after absorption of moisture. Good resistance to chemicals, dimensionally stable and low warpage. Heat-stabilised.	Stiff, dimensionally precise engineered parts for machine construction, the automotive industry and the electrical industry. Functional parts with system integration. Substitution of metal die-cast alloys.

Figure 2.5: Grivory GV-4H characteristics and properties

Grivory GV-4H Natural has excellent chemical resistance, is dimensionally stable, has low warpages, and is heat-stabilized. Grivory GV is particularly suited for the replacement of metal because to its high profile of qualities. The absorption of moisture has little effect on critical criteria for metal replacement, such as stiffness and strength. Grivory GV is physiologically safe and can be used in delicate applications such as food and drinking water.

Motorola Solution have machined the samples of Grivory GV-4H Natural based on given dimension for dog bone specimen. For this dog bone specimen, there will be

gauge length at the middle and shoulder area for gripping purpose. The gauge length of the dog bone specimen should have smallest cross-sectional area so that fracture will occur within the gauge length. To avoid unnecessary end effect from the shoulders. The length of transition between gauge section and shoulders section must be equal. There are 2 types of specimens which wanted to understand the flow of the fibre orientation of the specimens. Both of them are labelled as P (Parallel flow) and C (Cross flow). There are 10pcs for each flow direction. Total is 20pcs of P (Parallel flow) and C (Cross flow) specimens.
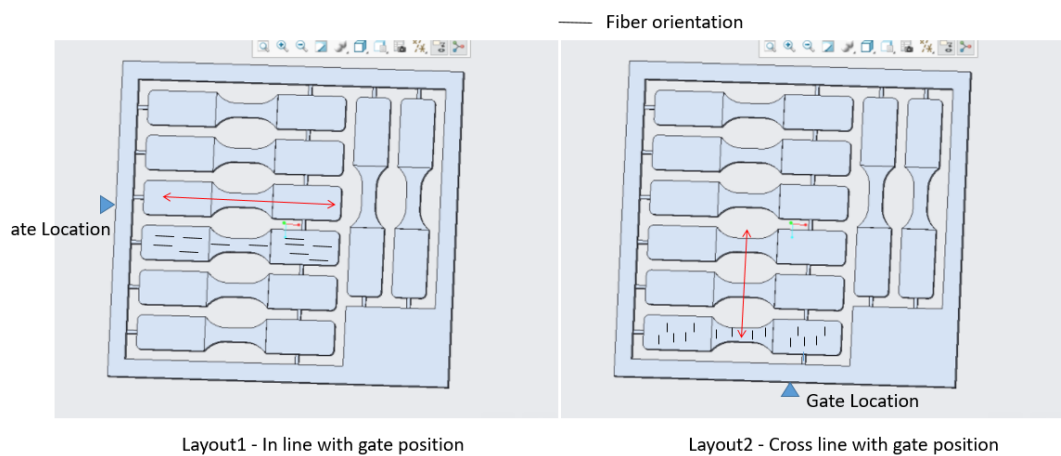

Figure 2.6: Parallel flow and Cross Flow of specimens

2.2   Pressure Vessel

Thin wall pressure vessels (TWPV) are commonly used in industry for the storage and transfer of liquids and gases. They're also found in aerospace and maritime vehicles including rocket and balloon skins, as well as submarine hulls. The walls of an ideal thin-walled pressure vessel act like a membrane, remaining unaffected by bending loads for the most of their length. Because it is the most structurally efficient shape, a spherical geometry is suitable for a closed pressure vessel. On the other hand, the cylindrical shape may be easier to construct and transport.

The fundamental precepts are wall thinness and geometric symmetry. These allow basic free-body diagrams to be used to analyse typical wall stresses (FBD).

1. In comparison to the vessel's other dimensions, the wall is said to be very thin. If the thickness is t and the characteristic size is R, assume that t/R 1, or R/t > 1. (For example, the radius of a cylinder). As a result, we can infer that the stresses are distributed evenly across the wall.

2. The geometry and loading of cylindrical vessels are cylindrically symmetric. As a result, the stresses are considered to be independent of the angular coordinate of the cylindrically coordinate system. Spherical vessels have spherically symmetric shape and loading. As a result, the stresses can be considered to be independent of the two angular coordinates of the spherical coordinate system and to be equal in all directions.

3. The internal pressure, denoted by p, is constant and always positive. If the vessel is also pressurised from the outside, such as by atmospheric pressure, p is computed by subtracting the external pressure from the gauge pressure. When the external pressure is higher, as it is in the case of a submarine hull, stress estimations should be utilised with caution because another failure mechanism, wall buckling, may be present.

4.   Features that could have an impact on the symmetry assumptions are ignored. Supports and end coverings for the cylinders are included. The idea is that basic stress state perturbations are localised and may be ignored in basic design decisions like lifting up the thickness away from such locations.

The cylinder has a radius of r and a thickness of t. The investigation's scope is limited to Thin-Walled Pressure Vessels. The radius to thickness (r/t) ratio of a cylinder must be at least 10 to qualify as "thin walled."

The thickness of the pressure vessel's walls is determined by the ratio of the vessel's mean radius to the thickness of the wall.
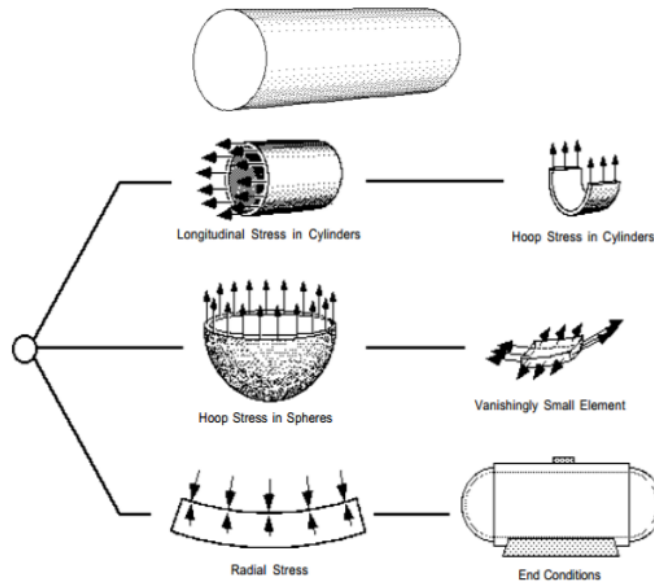
Figure 2.7: Stress in pressure vessel

$$\frac{r}{t} \geq 10$$

2.1

The vessel is classed as a thin-walled pressure vessel when this ratio surpasses ten. If the ratio is fewer than ten, the vessel is regarded as a thick wall pressure vessel.

radius = r
thickness = t
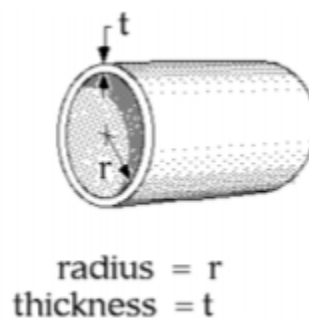
Figure 2.8: Classification of pressure vessel

In operation, the stresses created in a thin-walled pressure vessel's (thin) wall can be assumed to be uniform. The vast majority of pressure containers that power engineers will encounter are thin-walled.

A thick-walled pressure vessel, on the other hand, provides a greater (circumferential) stress on the inside surface, which reduces as the diameter approaches the outside.

A longitudinal cross-circumferential section's stress (or hoop stress) is computed as follows [15]:

$$\sigma_h = \frac{p d_m}{2t} \qquad\qquad 2.2$$

Where:

d_m = Mean diameter (Outside diameter - t)

p   = Internal pressure

t   = Wall thickness

σ_h = hoop stress

Longitudinal stress, as shown and deduced in the textbook, is calculated as follows:

$$\sigma_\approx = \frac{F}{A} = \frac{Pd^2}{(d + 2t)^2 - d^2} \qquad\qquad 2.3$$

Though a close approximation can be made

$$\sigma_\approx = \frac{Pd_m}{4t} \qquad\qquad 2.4$$

Where:

d_m = Mean diameter (Outside diameter - t)

p   = Internal pressure

t   = Wall thickness

$\sigma_\approx$ = Longitudinal stress

The internal pressure that is still pressing on this section of the cylinder is depicted in the pressure field below. During the cylinder's cut, the pressure remains constant. If the pressure acts in the other direction, as shown below, the following analysis should be utilised with caution. When we use "external pressure" to load vessels, the cylinder can buckle (crumple) as a result of the load.
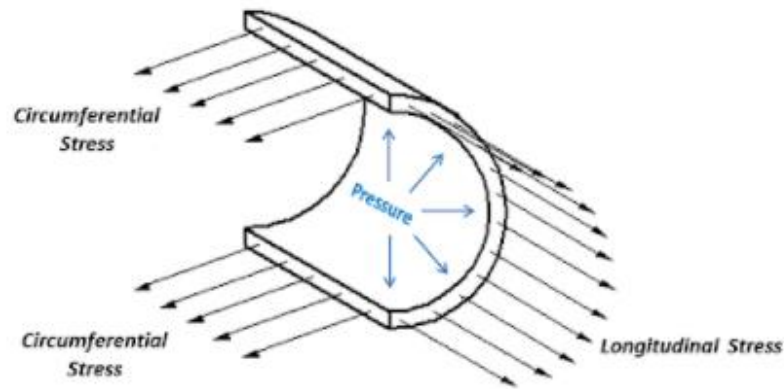
Figure 2.9: Stress inside pressure vessel

There must be some force counteracting the internal pressure in order for the figure to fulfil equilibrium. All stresses are assumed to act perpendicular to the vessel's surface when evaluating thin-walled pressure vessels. "Membrane activity" is the term for this. The normal stress σ_2 is the only stress that occurs on the cut in the cylinder below that may oppose the internal pressure.

There is sufficient information at this point to apply force equilibrium in a longitudinal direction. The force generated by internal pressure must be balanced by the force provided by longitudinal normal stress, as shown in the picture above.

σ_2 = Longitudinal Stress in Cylinder
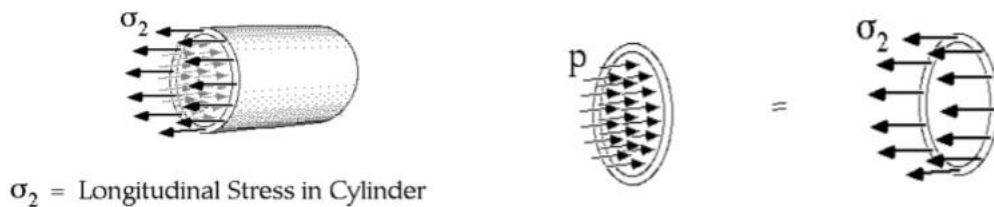
Figure 2.10: Internal pressure of pressure vessel

13

2.3 Methods of Pressure Vessel Testing

2.3.1 Visual Test (VT)

A visual inspection is one sort of assessment that can provide a good picture of a vessel's overall condition [16]. Pressure vessel inspectors will inspect every section of the vessel that they can view after confirming that the vessel's surface is clean. Welded seams will be checked, including those around appendages and along the length of the vessel's shell. They might notice cracks, corrosion, or erosion, or they might notice that the vessel appears to be in good working order. Visual inspections can help you spot some problems, but they only go so far.

2.4 Pressure Vessel Testing Benefits

Pressure vessel testing is required at certain stages, but it is also something that all manufacturers and end users should emphasize since it is vital to their operations and the safety of their employees. A failure in a pressure vessel containing a hazardous gas might result in a deadly gas release. A broken vessel can cause an explosion even if the substance within isn't dangerous.

An accident involving a pressure vessel could also result in catastrophic damage to nearby equipment. The expense of replacing the destroyed equipment might run into the hundreds of thousands, if not millions of dollars. According to OSHA, recent pressure vessel inspections have revealed that numerous pressure vessels in industries are damaged.

Regular inspections can help you avoid a dangerous breakdown. Pressure vessel inspection frequency varies depending on a variety of factors; however, we recommend inspecting pressure vessels every five years as a general rule. These checks should comprise a stress analysis, a visual inspection on the pressure vessel, a thickness evaluation on pressure vessel, a hydrostatic pressure test, and a check pressure release valve.

2.5   Split Hopkinson pressure bar (SHPB)

The Split-Hopkinson Pressure Bar (SHPB), commonly known as the Kolsky bar, is a high strain rate testing device. SHPB is ideal for high strain rate tests in the 10^2 to 10^4 s^{-1} range. Because these structures are subjected to dynamic stress, high strain rate data is essential for safety and structural integrity assessment.

Some of the most advanced methods for high strain rate material testing include the Split-Hopkinson Pressure Bar, plate impact test, Taylor impact, drop weight methods, cam plastometer and expanding ring technique. It was first used to detect dynamic pressure in 1914 by B. Hopkinson, who used a single elastic pressure bar with momentum traps at the end of the bar [17]. The pressures were created by explosives being detonated or bullets striking each other.

By addressing the pressure bar's constraints and presenting electrical assessment methods that permitted precise measurements of the pressure-time pulse passing through the bar, Davies made substantial advances to Hopkinson's theory. In 1949, Kolsky was the first to use two pressure bars. The incident (or input) and transmitter (or output) bars are two pressure bars with the same equal cross-sectional area that make up the SHPB.

A general Kolsky compression bar apparatus, as shown schematically in Figure 2.12, consists of three fundamental components: bar components, a loading device and a data collection and recording system.
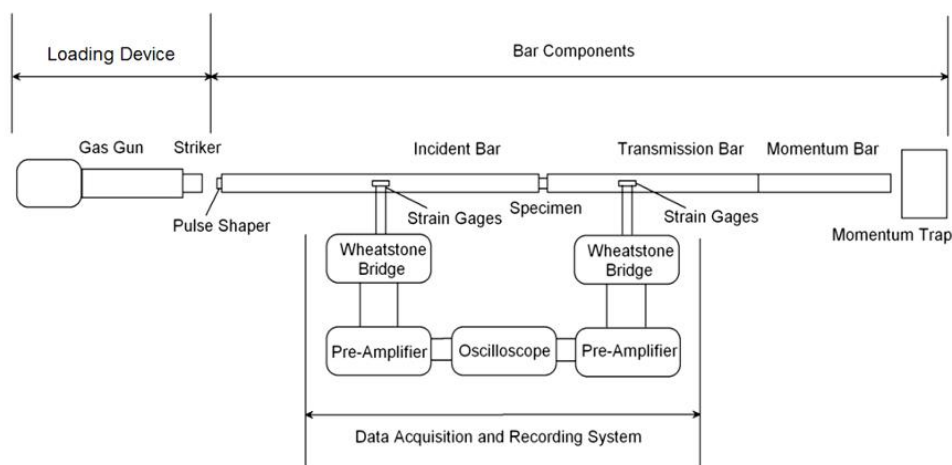

Figure 2.11: A Kolsky compression bar apparatus in general

Loading device: The loading in Kolsky-bar studies should be regulated, steady, and reproducible. The loading technique might be static or dynamic in most cases. The stored energy from the precompression is delivered into the originally unstressed portion of the incident bar when the clamp is quickly released. This causes a pressure wave to propagate towards the specimen in the incident bar. Kolsky compression bars have just lately been subjected to a sort of static loading. Dynamic loading, on the other hand, is becoming increasingly popular.

Kolsky's (1949) detonation method is an example of dynamic loading. In any case, firing a striker at the event bar is the most common method for dynamic loading. For Kolsky compression bars, gas guns have been demonstrated to be effective, controlled, and safe. The striker is fired by a fast release of pressurised air or a light gas from a pressure storage vessel, which accelerates in a long gun barrel until it collides with the end of the incident bar. So that the striker meets the incident bar at a constant speed, gas venting holes are made near the exit on the side of the gun barrel. The striking velocities are measured visually or magnetically just before the impact. With this style of striker launching system, the impact on the incident bar is controlled and repeatable. Changing the compressed gas tank pressure and/or the depth of the striker inside the gun barrel can essentially limit the striking speed. The length of the striker influences the loading time.

The bar material should be linearly elastic and have a high yield strength since surface strains are utilised to anticipate stress waves inside the bars. To allow one-dimensional wave propagation, the bars must be physically straight and free to move on their supports with minimal friction. The loading axis for the entire bar system should be adjusted along a single straight axis. The event bar should be at least twice the length of the striker to avoid overlapping between incident and reflected pulses. The specimen is placed between the event and transmission bars. The specimen axis is perpendicular to the common axis of the bar system.

Strain gauges have become a regular approach for quantifying bar strains in Kolsky-bar testing, according to the data gathering and recording system. Two strain gauges are usually linked uniformly across a bar diameter on the bar surface [18]. A Wheatstone bridge is used to adjust the signals from the strain gauges. In a conventional Kolsky-bar experiment, the voltage output from the Wheatstone bridge is of low amplitude, mainly on the range for milli-volts. A signal amplifier may be necessary to

accurately record the low-amplitude voltage using a high-speed or an A/D computer board oscilloscope. Both the amplifier and the oscilloscope in a typical Kolsky-bar experiment must have a sufficiently high frequency response to record the signal, which is typically less than one millisecond in duration. A data-acquisition system's components should all have a frequency response of at least 100 kHz.

2.5.1 Theory of SHPB

The young's modulus of the bar, E, and the density of the bar material, ρ_B, determine the sound speed in the bar material, C_B:

$$C_B = \sqrt{\frac{E}{\rho}}$$

2.5

The striker fires a "square wave" compression pulse into the incident bar for a time, Δt [19]. It is determined by the striker bar length, L_{st}:

$$\Delta t = \frac{2L_{St}}{C_B}$$

2.6

Likewise, the magnitude of the strain pulse, ε_i is determined by the striker's velocity.

$$\varepsilon_i = \frac{v_{st}}{2C_B}$$

2.7

The average engineering strain rate in the specimen is the variation in velocity across the specimen divided by the gauge length of the specimen, L_S.

$$\dot{\varepsilon} = \frac{v_1 - v_2}{L_s}$$

2.8

The velocity of the striker determines the specimen strain rate. The strain gauge positioned on the incident bar can be used to determine the stresses generated when the striker collides with the incident bar. Johnson's two equations link the stress in the striker, σ_{st}, and incident bar, σ_i to the velocity in the common interface [20]:

$$\sigma_{st} = \rho_{st} C_{st} (v_{st} - v_i) \qquad 2.9$$

$$\sigma_i = \rho_B C_B v_i \qquad 2.10$$

The striker's response force is equal to the force exerted on the incident bar during impact:

$$F_{st} = F_i \qquad 2.11$$

$$A_{st} \sigma_{st} = A_B \sigma_i \qquad 2.12$$

Substituting equation 2.9 and 2.10 into equation 2.12 gives:

$$A_{st} \rho_{st} C_{st} (v_{st} - v_i) = A_B \rho_B C_B v_I \qquad 2.13$$

$$\beta = \frac{A_{st} \rho_{st} C_{st}}{A_B \rho_B C_B} \qquad 2.14$$

To permit one-dimensional wave propagation, the striker bar and incident bar must have the same features and cross-sectional areas, yielding $\beta=1$. As a result, we may rewrite equation 2.13 as:

$$v_i = \frac{\beta v_{st}}{1 + \beta} = \frac{v_{st}}{2} \qquad 2.15$$

Substituting equation 2.15 into equation 2.9 and equation 2.10 gives:

$$\sigma_{st} = \rho_B C_B \left(v_{st} - \frac{v_{st}}{2}\right) = \frac{\rho_B C_B v_{st}}{2} \qquad 2.16$$

$$\sigma_i = \rho_B C_B \left(\frac{v_{st}}{2} \right) \qquad\qquad 2.17$$

Similar to the interaction between the striker and incident bars, the force exerted on the specimen is equal to the reaction force exerted on the incident bar, assuming no losses:

$$F_i = F_s \qquad\qquad 2.18$$

Remember that the stress pulse is both transmitted and reflected at this interface, thus the transmitted and reflected stress pulses are:

$$A_B \sigma_t = A_s \sigma_s \qquad\qquad 2.19$$

$$\sigma_t = \frac{A_s \sigma_s}{A_B} \qquad\qquad 2.20$$

$$\sigma_r = E_B \epsilon_r \qquad\qquad 2.21$$

where "σ_r" denotes reflected stress, "σ_t" denotes transmitted stress, and "A_S" for the specimen's cross-sectional area.

$$\sigma_r = \frac{E_B L_s}{-2C_B} \dot{\varepsilon} \qquad\qquad 2.22$$

As the difference between reflected stress and incident equals transmitted stress, so incident stress equals:

$$\sigma_i = \sigma_t - (-\sigma_r) \qquad\qquad 2.23$$

Substituting equations 2.20 and 2.22 into equation 2.23 gives:

$$\sigma_i = \frac{A_s \sigma_s}{A_B} + \frac{E_B L_s}{2C_B} \dot{\varepsilon} \qquad\qquad 2.24$$

And substituting equation 2.24 into equation 2.17 gives:

$$V_{st} = \frac{2}{\rho_B C_B}\left(\frac{A_S}{A_B}\sigma_S + E_B\frac{L_S\dot{\varepsilon}}{2C_B}\right)$$ 2.25

Equation 2.25 gives the result of the striker velocity so that a specific strain rate and stress level in the specimen can be achieve.

2.6 Universal Tensile Machine (UTM)

A universal testing machine can be used to apply a tensile force to a sample specimen and estimate different properties of the specimen under stress. The quasi static test is done on a universal testing machine at 1 mm/min tensile strain rates until the specimen breaks (yields or even breaks) [21]. Despite the fact that universal testing machines can measure a wide range of tensile properties, the most well-known tensile properties are tensile strength and tensile modulus. The maximum amount of force that a plastic can withstand before it breaks. Tensile modulus, on how much a material may deform due of stress prior it yields. The modulus of a material is a measurement of its stiffness. Elongation is calculated by dividing the expansion in gauge length following a break by the original gauge length. Ductility is indicated by the lengthening of the fibres. The Poisson's Ratio is a measurement of how far a material is stretched and how thin it becomes as a result of that stretching.

2.7 Scanning Electron Microscopy (SEM)

The scanning electron microscope (SEM) creates a variety of signals on the surface of solid specimens using a focused beam of high-energy electrons [22]. Interactions between electrons and the sample provide signals that transmit information about the sample's exterior appearance, chemical composition, and crystalline structure and orientation of the components that make it up [23]. Data is collected over a defined area of the sample's surface in various applications, and a 2-dimensional picture is generated to demonstrate spatial variations in these attributes. In scanning mode, regions ranging from 1 cm to 5 microns in width can be scanned using typical SEM techniques. The SEM can be used to look at specific point locations on a sample; this method is very effective for evaluating crystalline structure, crystal orientations chemical compositions and in a semi-quantitative manner.

Figure 2.13 show an operating mechanism of SEM machine [24]. An electron gun will produce beam of electron at the top of microscope. These beams of electron will follow vertical path of microscope through the electromagnetic fields and lenses. The X-rays and electrons are ejected from the sample/specimen as the beam hit the sample/specimen. The detectors will then collect these backscattered electron, X-rays and secondary electron which will convert them into a signal. This signal will send to screen monitor and the final image is produced. SEM can be conducted at low (50-100×) and medium (200-500×) magnification levels. Low magnification photos gave a broad pattern of the cross-section since SEM covered a larger area in each shot.
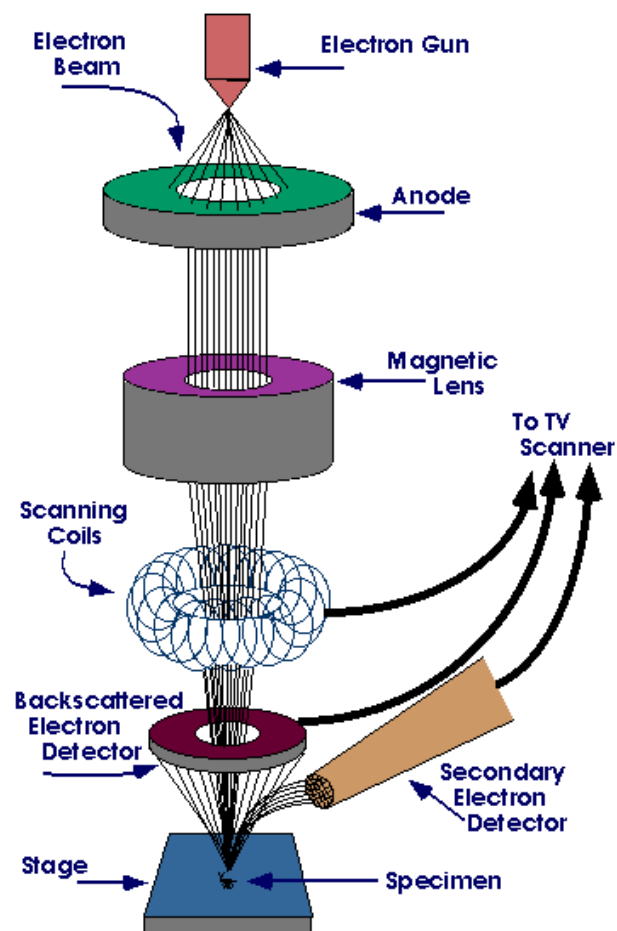

Figure 2.12: Operating mechanism of SEM Machine

This magnification level is used to determine the length of the specimen's existing flaws. The photos from this level were stitched together to create a panoramic image of all of the sections. High-level magnification imaging was primarily used to

21

monitor the single glass fibres after medium-level magnification photographs offered a more detailed look of the section.

2.8   Image Processing

Image processing has become one of area of study in many industries. Image J is a software that helps to do image processing process. Programming based on algorithms used to perform image processing on digital images [25]. Image J is Java based, free ware and one of most popular applications for image processing purpose beside MATLAB. This software is originally developed by National Institutes of Health at Unites Stated. In image J, morphology of particles distributions, size distribution and particle size can be analysed. Besides that, image J also can be used for analysing data of scattering intensity data which will help to find size of particles. Image J consists of several important steps of image acquisition, filtration and segmentation. From the original image, Gaussian function and median function of filtration techniques will used to generate new image. This new image will then be converted to binary image where segmentation is used to separate the particles of overlapping. Thus, it'll give accurate result of the particles shapes.

CHAPTER 3 : Methodology

3.1   Compressed Air Tank

Compressed air tank or thin wall pressure vessel (TWPV) was built according to the specification given. Below figure is datasheet for welded steel pipe used to build compressed air tank [26].

Welded Steel Pipes : Medium Series (M)
MS 863 : 2010 / BS EN 10255 : 2004 / BS 1387 : 1985 (B) / MANUFACTURER'S STANDARD

| NOMINAL DIAMETER DN | SPECIFIED OUTSIDE DIAMETER D | THREAD SIZE R | OUTSIDE DIAMETER | | WALL THICKNESS T | CALCULATED MASS | | NUMBER OF THREADS PER INCH | SOCKET LENGTH | TEST PRESSURE |
| | | | max | min | | PLAIN END | THREADED & SOCKETED | | min | |
mm	mm		mm	mm	mm	kg/m	kg/m		mm	BAR
15	21.3	½	21.8	21.0	2.6	1.21	1.22	14	34.0	50
20	26.9	¾	27.3	26.5	2.6	1.56	1.57	14	37.0	50
25	33.7	1	34.2	33.3	3.2	2.41	2.43	11	43.0	50
32	42.4	1 ¼	42.9	42.0	3.2	3.10	3.13	11	48.0	50
40	48.3	1 ½	48.8	47.9	3.2	3.56	3.60	11	52.5	50
50	60.3	2	60.8	59.7	3.6	5.03	5.10	11	62.5	50
65	76.1	2 ½	76.6	75.3	3.6	6.42	6.54	11	71.5	50
80	88.9	3	89.5	88.0	4.0	8.36	8.53	11	77.0	50
100	114.3	4	115.0	113.1	4.5	12.20	12.50	11	91.0	50
125	139.7	5	140.8	138.5	5.0	16.60	17.10	11	105.5	50
150	165.1	6	166.5	163.9	5.0	19.80	20.40	11	116.5	50

Figure 3.1: Manufacturer's standard for Welded Steel Pipes: Medium Series (M)
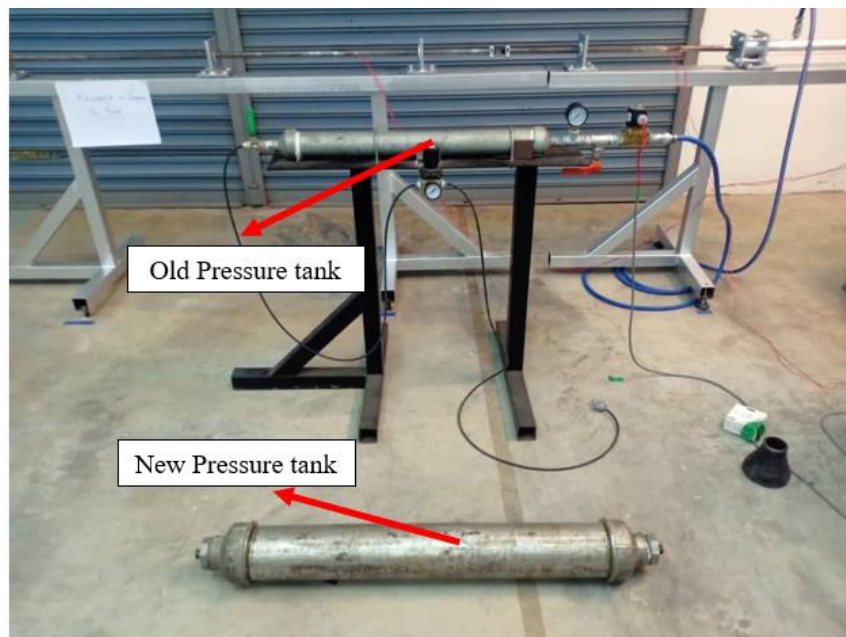

Figure 3.2: Changing the old pressure tank to new pressure tank

3.2   Compressed Air Tank Testing

Figure 3.3: Gas leaking is found on the pipe joint using visual inspection technique

Figure 3.4: Gas leakages is solve using epoxy resin

Based on figure 3.3, there is some gas leaking from the pressure pipe. This can cause pressure drop very rapidly, thus SHPB tensile test result will not be favourable. By using visual inspection techniques, after applying soap water on the surface and joint of pressure vessel, there are some bubbles come out. The epoxy resin is applied on the pipe to reducer socket and reducer socket to reducer nipple. This epoxy resin will harden when it's cure. Epoxy resin glue is basically design to create permanent seal or bonding and it's a long lasting compare to Teflon tape.